PCCP

Dynamic Article Links

Cite this: *Phys. Chem. Chem. Phys.*, 2012, **14**, 7304–7308

www.rsc.org/pccp

PAPER

Electronic structures of one-dimensional metal–molecule hybrid chains studied using scanning tunneling microscopy and density functional theory†

Kyung-Hoon Chung,‡[a] Bon-Gil Koo,‡[b] Howon Kim,[a] Jong Keon Yoon,[a] Ji-Hoon Kim,[b] Young-Kyun Kwon*[b] and Se-Jong Kahng*[a]

Received 19th October 2011, Accepted 26th March 2012
DOI: 10.1039/c2cp23295b

The electronic structures of self-assembled hybrid chains comprising Ag atoms and organic molecules were studied using scanning tunneling microscopy (STM) and spectroscopy (STS) in parallel with density functional theory (DFT). Hybrid chains were prepared by catalytic breaking of Br–C bonds in 4,4″-dibromo-*p*-terphenyl molecules, followed by spontaneous formation of Ag–C bonds on Ag(111). An atomic model was proposed for the observed hybrid chain structures. Four electronic states were resolved using STS measurements, and strong energy dependence was observed in STM images. These results were explained using first-principles calculations based on DFT.

I. Introduction

Metal–organic hybrid structures have received considerable attention because of their engineerable electronic, magnetic, and catalytic properties.[1–6] They can be grown by surface-confined spontaneous processes in a vacuum environment, and visualized by scanning tunneling microscopy (STM) techniques.[7–9] The hybrid structures grown by using halogenated carbon ligands became a focus of recent studies.[10–15] It has been known that weak C–I and C–Br bonds (2.4 and 3.0 eV, respectively)[16] in organic molecules are easily broken and thus unpaired electrons are exposed in C atoms inducing subsequent coupling reactions on metal surfaces. Such molecular processes have been studied in iodobenzene on Cu(111) using surface-sensitive techniques under vacuum conditions, such as temperature-programmed reaction (TPR), high resolution electron energy loss spectroscopy (HREELS), and near-edge X-ray fine structure spectroscopy (NEXAFS).[17–19] It has been suggested that intermediate states, different from covalently bonded structures, emerge between 170 and 300 K. Recent STM studies showed that a chain-like structure formed when diiodobenzenes were exposed on Cu(111) and Cu(110) at room temperature.[10–12] It is explained that a Cu-mediated catalytic reaction converts each diiodobenzene into a phenylene group by removing two iodine atoms, and then creates hybrid chains consisting of Cu-phenyl units. Similar mechanisms have been used to prepare 1- and 2-dimensional metal–organic hybrid structures on metal surfaces.[9,13,14] These studies were mostly performed on Cu surfaces, but the experiments on Ag(111) with 9,10-dibromoanthracene molecules were reported by our group.[15] To understand the physical properties of these hybrid structures, their electronic structures need to be investigated. However, no study on such electronic structures is available in the literature.

In this paper, we report our study on the geometric and electronic structures of metal–organic hybrid chains using STM and scanning tunneling spectroscopy (STS), in tandem with first-principles density functional theory (DFT) calculations. Hybrid chains were grown by the deposition of 4,4″-dibromo-*p*-terphenyl (DBTP) on Ag(111) at 300 K. We observed several electronic states in STS measurements and strong energy dependence in STM images, which were accounted for by our first-principles calculations.

II. Experiment

All STM experiments were performed using a home-built STM housed in an ultrahigh vacuum (UHV) chamber with a base pressure below 7×10^{-11} Torr. An Ag(111) single crystal was cleaned by several cycles of Ne-ion sputtering and annealing at 800 K for 40 min. The surface cleanliness was checked by STM observation of an atomically-flat Ag(111) surface. Commercially available 4,4″-dibromo-*p*-terphenyl (Tokyo Chemical Industry, Japan) was thermally evaporated onto the Ag(111) surface with submonolayer coverage from an

[a] *Department of Physics, Korea University, 1-5 Anam-dong, Seongbuk-gu, 136-713, Seoul, Korea. E-mail: sjkahng@korea.ac.kr*
[b] *Department of Physics and Research Institute for Basic Sciences, Kyung Hee University, 130-701, Seoul, Korea. E-mail: ykkwon@khu.ac.kr*

† Electronic supplementary information (ESI) available. See DOI: 10.1039/c2cp23295b

‡ These authors equally contributed to this work.

alumina-coated crucible while keeping the substrate temperature at 300 K. The DBTP molecules were degassed for several hours prior to the deposition. The prepared sample was transferred to the STM and cooled to 80 K. STM images were obtained at constant-current mode with a Pt/Rh tip. STS spectra were obtained using a lock-in detection technique with a modulation voltage of 8 mV (rms) and at a frequency of 1.7 kHz. A feedback loop was opened for STS measurements.

III. Calculation

To investigate the structural and electronic properties of the (Ag–Terphenyl)$_n$ hybrid chain on the Ag(111) surface and analyze its STM images, we performed *first-principle* calculations within the DFT framework. We used the Perdew–Burke–Ernzerhof (PBE) parametrization[20] of the generalized gradient approximation (GGA) for the exchange–correlation functional to DFT, as implemented in the SIESTA code.[21] The behavior of valence electrons was described by norm-conserving Troullier–Martins pseudopotentials[22] in the Kleinman–Bylander factorized form.[23] Especially for Ag atoms, scalar-relativistic effects were included. An atomic orbital basis with a double-ζ polarization was used to expand the electronic wave functions. The charge density and potentials were determined on a real-space grid with a mesh cutoff energy of 210 Ry. We used a confinement energy shift of 0.01 eV, which defines the cutoff radii of the atomic orbitals. All geometries were optimized without any symmetry constraints using the conjugate gradient method[24] until none of the residual Hellmann–Feynman forces acting on any atom would exceed 1.0×10^{-3} Ry a_B^{-1}, where a_B is the Bohr radius. We complemented the Ag basis by including initially unoccupied 5p orbitals.

IV. Results and discussion

Fig. 1(a) shows the chemical structure of a DBTP molecule and the expected reaction on the Ag(111) surface at 300 K. The molecule has three phenyl rings terminated by two Br atoms. Fig. 1(b) and (c) show STM images obtained at 80 K after DBTP was deposited on the substrate at 300 K. We observed well-ordered 2D islands made of parallel molecular chains separated by paired balls. We assigned the chains and the balls as (Ag–Terphenyl)$_n$s and Br atoms, respectively. Similar to the diiodobenzene reactions on Cu surfaces, Br atoms are detached from DBTP molecules to produce terphenyl (TP) biradicals. The TPs take Ag atoms to form C–Ag–C coordination bonds, resulting in (Ag–TP)$_n$ hybrid chains. Ag atoms could be seized from mobile adatoms, or pulled from the surface layer during the reaction. 2-Dimensional adatom gas forms on both Ag(111) and Cu(111) surfaces at 300 K with competing attachment and detachment kinetics at step edges.[25–28] Catalytic activity of Ag(111) was previously studied in the bond breaking of C–I from iodobenzene and other I-containing molecules below 300 K using temperature programmed desorption (TPD) and X-ray photoelectron spectroscopy (XPS).[29–31] STM experiments also showed that hybrid chain formation occurred in 9,10-dibromoanthracene on Ag(111).[15] In contrast, it was reported that 1,3,5-tris(4-bromophenyl)-benzene did not undergo dehalogenation on Ag(111).[13]

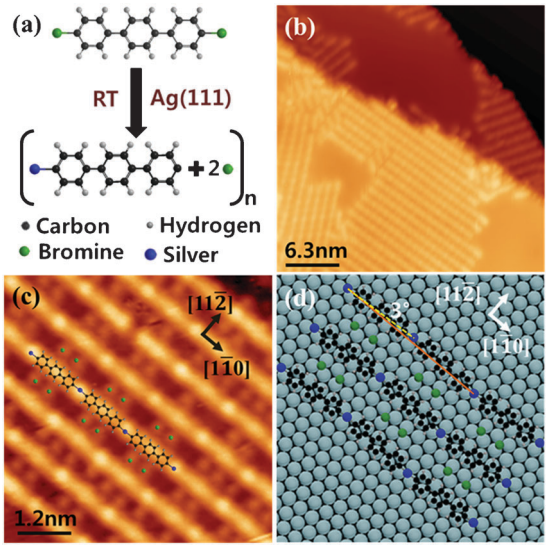

Fig. 1 (a) Chemical structures of a 4,4″-dibromo-*p*-terphenyl (DBTP) molecule and schematic of the catalytic reactions. (b) Typical STM image measured at 80 K after DBTP molecules were deposited at room temperature on Ag(111). A 2D island was made of 1D hybrid chains of Ag–TP. Size of STM image: 31.5×31.5 nm^2, sample bias: $V_S = 1.0$ V. (c) STM image zoomed in on an island. The molecular model of the Ag–TP chain was superimposed. Size of STM image: 6×6 nm^2, sample bias: $V_S = 0.5$ V. (d) Atomic model made for three parallel hybrid chains (black: carbon, gray: hydrogen, green: bromine, blue: silver). Tunneling current: $I_T = 0.1$ nA.

This implies that there are additional factors that determine the catalytic activity of surfaces. For example, there can be preferred adsorption configurations of molecules, C–Br bonds, and Ag adatoms to effectively trigger dehalogenation and subsequent chain formation.

The Ag–TP hybrid chains were observed along three equivalent crystallographic directions, [1$\bar{1}$0], [10$\bar{1}$], and [01$\bar{1}$]. The average distance between two adjacent hybrid chains was 1.00 nm ± 0.05 nm, corresponding to 2 Ag lattices (1.00 nm) along [11$\bar{2}$]. The average distance of Ag–TP–Ag in a hybrid chain was 1.59 nm ± 0.05 nm, corresponding to 5.5 Ag (1.59 nm) lattices along [1$\bar{1}$0], which was slightly longer than the length of a DBTP molecule, 1.52 nm. Based on these observations, an atomistic model structure was made as shown in Fig. 1(d). Ag atoms adsorbed alternately on face-centered cubic (fcc) and hexagonal close-packing (hcp) hollow sites, forming a zigzag chain with the axes of TPs tilted by a tilt angle of ~3° from the direction of the chain axis along [1$\bar{1}$0]. The centers of three hexagon rings in a TP–Ag unit locate at bridge sites, and Br atoms locate at hollow sites between two parallel hybrid chains, especially in the middle of four hydrogen atoms. We believe that they were stabilized by weak electrostatic interactions between H and Br.[15]

To reveal electronic structures of the hybrid chains, STS measurements were performed. Fig. 2(c) shows STS curves obtained at three locations of a molecular chain: the Ag, the TP, and the end of the chain (marked in Fig. 2(a)). STS data obtained from single and 2D self-assembled hybrid chains showed similar results. Molecular distance was too far (1 nm) to have significant modification in electronic structures.

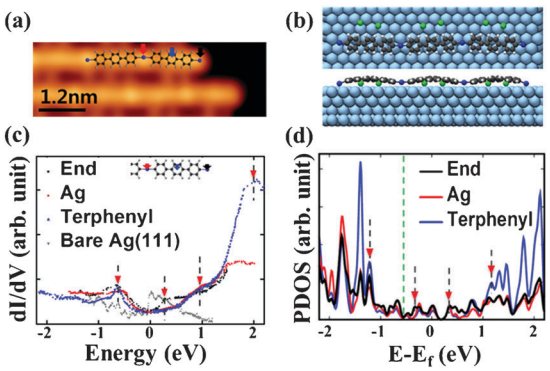

Fig. 2 (a) High-resolution STM image of hybrid chains. Size of STM image: 6×1.9 nm^2, sample bias: $V_S = -0.6$ V, tunneling current: $I_T = 0.1$ nA. (b) Top and side views of the optimized structure of the hybrid chains on the Ag(111) substrate obtained by the DFT calculation. (c) Site-dependent STS (dI/dV) spectra marked with the different colored arrows in (a) (black: end of chain, blue: TP inside chain, red: Ag atom inside chain). Initial tunneling conditions are $I_T = 0.1$ nA and $V_S = 0.6$ V. (d) Calculated PDOS of $(Ag–TP)_3$ performed at corresponding sites with experimental STS spectra (c) (black: end of chain, blue: TP inside chain, red: Ag atom inside chain). The green dashed line is regarded as the Fermi level observed experimentally, while zero corresponds to the calculated Fermi level.

The site-dependent STS spectra revealed local electronic characteristics of a hybrid chain. Four major peaks were observed in the three spectra. All the three spectra had a peak at -0.6 eV. Only the spectrum from the end of a chain had a peak at $+0.3$ eV. The spectra from the TP and the mid-chain Ag had peaks at $+0.8$ eV. The spectrum from the TP had a peak at $+2.0$ eV.

To understand the observed structures and their electronic states, we performed first-principles calculations based on DFT. Our studies address both infinite and finite metal–molecule hybrid chains on the Ag(111) surface. Four layers of Ag atoms were employed in the calculations and Ag atoms in the two bottom layers were fixed in space to simulate the Ag(111) substrate. To describe a small tilt angle ($\sim 3^\circ$) seen in our STM images (Fig. 1(c) and 2(a)) and shown in the model structure (Fig. 1(d)), we used two formula units of the Ag–TP compound in a unit cell for infinite hybrid chains, whereas $(Ag–TP)_2$ and $(Ag–TP)_3$ structures were used in a supercell for finite chains. Finite chains were considered to analyze the effect of the Ag end atoms. Two Br atoms removed from the original DBTP molecule were placed near the hybrid chain. We used 242 atoms in a unit cell for the infinite hybrid chain on the Ag substrate, and 404 atoms for the finite $(Ag–TP)_3$ chain on the Ag substrate. To verify if our model structure is truly in equilibrium, we performed the structural relaxation based on the conjugated gradient method with different initial configurations and compared the energy of each structure with that of the structure described above. (See the ESI† for detailed results.) We found that the most stable structure obtained computationally was essentially the same as the structure observed in our STM measurements.

Fig. 2(b) shows the optimized structure of a finite $(Ag–TP)_3$ chain with an extra Ag atom at one end on the Ag(111) substrate. The top view shows the axes of TPs zigzagging by 3° from the chain axis along the $[1\bar{1}0]$ direction. Ag atoms are located alternately on fcc and hcp hollow sites in agreement with the model of Fig 1(d). The side view shows that TP parts are concaved down to match the unit chain length with the length provided by the Ag substrate. We obtained a similar equilibrium structure also for infinite hybrid chains.

To examine whether the zigzagging and concaving-down configuration is due to the effect of the Ag substrate or not, we calculated the equilibrium structures of the isolated (without the Ag substrate) infinite Ag–TP chain with two formula units in the unit cell while changing its axial lattice constant (see Fig. S1(a) of the ESI†). Quite surprisingly, even an isolated chain prefers not only the zigzag structure, but also the TP part to be concaved down similar to that on the substrate. The tilt angle of the axes of the TPs from the chain axis is about 5.4°, even bigger than $\sim 3^\circ$ observed on the Ag substrate. Moreover, three phenyl rings within a formula unit are twisted alternately, which appears to reduce the repulsive interaction between two H atoms located in neighboring phenyl rings. This equilibrium chain structure was found to be more stable by about 0.2 eV than its straight and flat counterpart. Therefore, the chain on the Ag substrate becomes stretched a little due to strong binding of the Ag atoms on the Ag substrate resulting in less tilting and twisting. We also found that this hybrid chain structure was more stable on the Ag substrate than adsorbed DBTP structures (and Ag adatoms) without reactions with the energy gain of about 1.6 eV per formula unit.

Fig. 2(d) shows the projected densities of states (PDOS) onto the Ag end atom, the Ag atom in between two neighboring TPs, and the TP calculated from a finite hybrid chain with three formula units terminated with Ag atoms. Considering the size of the STM tip, we included some contributions from neighboring parts into PDOS calculations. Before we analyze our calculated PDOS by comparing with the experimental STS data, we first calculated the DOS of the isolated hybrid chains. Both finite and infinite isolated chains present clearly a state at their Fermi level E_F and an energy gap of about 2.5 eV up to the lowest unoccupied state (see Fig. S1(b) of the ESI† for an infinite chain). We found that such an energy gap corresponds to the energy difference between the two peaks at -1.3 eV and $+1.2$ eV in Fig. 2(d) due to an electron transfer from the Ag substrate to the hybrid chain shifting E_F relatively to higher energy for the hybrid chain. According to our Mulliken population analysis,[32] the amount of electron transfer was 1.92 e per formula unit of the hybrid chain. In the energy gap, isolated chains did not have any state, but the hybrid chains on Ag(111) showed additional small peaks in Fig. 2(d). They originate from hybridization between the Ag substrate and the hybrid chain.

Taking into account the fact that the calculated Fermi level may differ from the experimentally measured value, our calculated PDOS in Fig. 2(d) are in good agreement with the measured STS data in Fig. 2(c). This difference may occur due to various reasons such as atomic defects and subsurface impurities. Assuming that the calculated E_F is off by 0.6 eV, that is, the Fermi level is located where the green dashed line is drawn in Fig. 2(d), we identified that four peaks have one-to-one correspondence with the four states observed in experiments.

They are marked with arrows in Fig. 2(c) and (d). First, the calculated states at about −1.4 to −1.2 eV correspond to the experimentally observed states at −0.6 eV. These states were degenerated states and spread anywhere in hybrid chains, which is in agreement with the fact that they were observed at all three points, TP, mid- and end-chain Ag in experiments. Second, the calculated state at −0.3 eV corresponded to the experimentally observed states at +0.3 eV. In both the calculations and experiments, they were found at ends of hybrid chains. Next, the calculated states at +0.3 eV corresponded to the experimentally observed states at +0.8 eV. They appeared at all three regions in the calculations, but mostly at TPs and Ag atom in the experiments. Finally, the calculated states around +1.2 to +1.4 eV corresponded to the experimentally observed states at +2.0 eV. They were contributed from the TPs. Although STS data at mid-Ag and end locations did not cover +2.0 eV, we were able to confirm, in dI/dV images, that TPs were much brighter than others at +2.0 eV. Other than that, calculated electronic states are in good agreement with the experimental results. In our calculations, Br atoms were included and had a state only at high bias ($>|1.8|$ eV) that did not overlap with the molecular states of hybrid chains. Therefore, it is reasonable to deduce the properties of self-assembled hybrid chains from the results obtained from single hybrid chains. Note that there are other peaks in Fig. 2(d) that we did not discuss. These peaks, as we mentioned above, are mainly due to the hybridization with the Ag substrate, and spatially distribute in-between Ag atoms and TP radicals.

We also obtained STM images at different energy levels from the same area of hybrid chains. They showed strong energy dependence in Fig. 3(a)–(d), which was clearly reproduced by simulated STM images in Fig. 3(e)–(h). To clarify the variation, one model molecule was overlaid in STM images, and cross-sections along four lines denoted in Fig. 3(a)–(d) are plotted in Fig. 3(i). Similarly, the calculated height profiles are shown in Fig. 3(j). At −0.6 V, the apparent height of the TP was smaller than that of Ag. The STM image consists of integration of energy states from the Fermi level. So although both the TP and Ag had electronic states observed in experiments and calculations, Ag had a slightly higher sum of density of state in the STS data that makes the apparent height of Ag higher than TP. With increasing energy, the apparent height of TP gradually increased, and became much greater than that of Ag at +2.0 V. So, at low energies below +0.8 V, Ag atoms looked brighter than TP, while TP looked brighter than Ag at high energies. This increase in the apparent height of TP at high energies was caused by the two states observed at +0.8 V and +2.0 V. Therefore, the observed energy-dependent STM images are consistent with STS data, and qualitatively well-reproduced by simulated STM images.

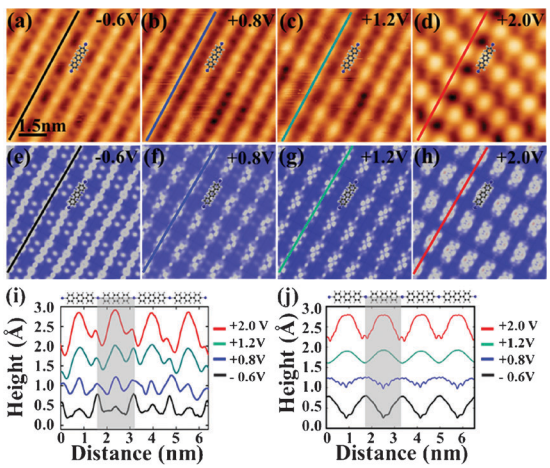

Fig. 3 Energy dependent STM images obtained at (a) −0.6 V, (b) +0.8 V, (c) +1.2 V and (d) +2.0 V. (a)–(d) Sizes of STM images: 7.5 × 7.5 nm^2, tunneling current: I_T = 0.1 nA. And corresponding simulated STM images obtained at (e) −0.6 V, (f) +0.8 V, (g) +1.2 V and (h) +2.0 V. The profiles along the hybrid chain denoted in the (i) experimental STM images in (a)–(d) and in the (j) simulated STM images in (e)–(h). The red line is the profile obtained at +2.0 V, cyan is the profile at +1.2 V, blue is the profile at +0.8 V and black is the profile at −0.6 V.

Recently, a similar observation using the same molecule on a different surface, Cu(111), was reported by W. Wang *et al.*[33] Hybrid chains of straight (Cu–TP)$_n$ were observed on Cu(111) with a little longer Cu–TP–Cu distance (1.62 nm) than our zigzagging Ag–TP–Ag (1.59 nm). The dI/dV values obtained at TP location remained higher than those at Cu for the energies below 1.8 eV, implying that there would be no energy-dependent height inversion, observed in our STM images.

V. Conclusion

In summary, we prepared metal–organic hybrid chains *via* spontaneous catalytic reactions on Ag(111). An atomic model consisting of Ag, TP, and Br with zigzagging structure was proposed. Four electronic states were resolved in site-dependent STS measurements and strong energy dependence was observed in STS and STM images. The atomic model, electronic states in STS, and energy dependent STM images were clearly reproduced by first-principles calculations, explaining the geometric and electronic structures of the hybrid chains. Our study illustrates that the local electronic structures of low-dimensional hybrid structures can be probed by the combined effort of STS and DFT studies. These approaches can be used to characterize more hybrid structures grown by catalytic reactions with variety of molecules and substrates providing a powerful tool to understand their geometric and electronic structures.

Acknowledgements

The authors gratefully acknowledge financial support from the National Research Foundation of Korea, and from the Ministry of Education, Science and Technology of the Korean government (Grant no. 2007-0054038, 2010-0025301, 2010-0018781, 2011-0002456, and 2011-0016188). Some portion of our computational work was done using the resources of the KISTI Supercomputing Center (KSC-2011-C1-04 and KSC-2011-C1-19).

References

1 L. R. MacGillivray, *Metal-Organic Frameworks: Design and Application*, John Wiley & Sons Inc., Hoboken, USA, 2010.
2 N. W. Ockwig, O. Delgado-Friedrichs, M. O'Keeffe and O. M. Yaghi, *Acc. Chem. Res.*, 2005, **38**, 176.
3 G. Férey, *Chem. Soc. Rev.*, 2008, **37**, 191.

4 S. T. Meek, J. A. Greathouse and M. D. Allendorf, *Adv. Mater.*, 2011, **23**, 249.
5 A. Carné, C. Carbonell, I. Imaz and D. Maspoch, *Chem. Soc. Rev.*, 2011, **40**, 291.
6 D. Zacher, R. Schmid, C. Wöll and R. A. Fischer, *Angew. Chem., Int. Ed.*, 2011, **50**, 176.
7 P. Gambardella, *et al.*, *Nat. Mater.*, 2009, **8**, 189.
8 J. V. Barth, *Surf. Sci.*, 2009, **603**, 1533.
9 M. Lackinger and W. M. Heckl, *J. Phys. D: Appl. Phys.*, 2011, **44**, 464011.
10 E. C. H. Sykes, P. Han, S. A. Kandel, K. F. Kelly, G. S. McCarty and P. S. Weiss, *Acc. Chem. Res.*, 2003, **36**, 945.
11 G. S. McCarty and P. S. Weiss, *J. Am. Chem. Soc.*, 2004, **126**, 16772.
12 J. A. Lipton-Duffin, O. Ivasenko, D. F. Perepichka and F. Rosei, *Small*, 2009, **5**, 592.
13 H. Walch, R. Gutzler, T. Sirtl, G. Eder and M. Lackinger, *J. Phys. Chem. C*, 2010, **114**, 12604.
14 C. J. Villagómez, T. Sasaki, J. M. Tour and L. Grill, *J. Am. Chem. Soc.*, 2010, **132**, 16848.
15 J. Park, K. Y. Kim, K.-H. Chung, J. K. Yoon, H. Kim, S. Han and S.-J. Kahng, *J. Phys. Chem. C*, 2011, **115**, 14834.
16 S. Samukawa, T. Mukai and K.-i. Tsuda, *J. Vac. Sci. Technol., A*, 1999, **17**, 2551.
17 M. Xi and B. E. Bent, *Surf. Sci.*, 1992, **278**, 19.
18 M. Xi and B. E. Bent, *J. Am. Chem. Soc.*, 1993, **115**, 7426.
19 M. X. Yang, M. Xi, H. Yuan, B. E. Bent, P. Stevens and J. M. White, *Surf. Sci.*, 1995, **341**, 9.
20 J. P. Perdew, K. Burke and M. Ernzerhof, *Phys. Rev. Lett.*, 1996, **77**, 3865.
21 J. M. Soler, E. Artacho, J. D. Gale, A. García, J. Junquera, P. Ordejón and D. Sánchez-Portal, *J. Phys.: Condens. Matter*, 2002, **14**, 2745.
22 N. Troullier and J. L. Martins, *Phys. Rev. B*, 1991, **43**, 1993.
23 L. Kleinman and D. M. Bylander, *Phys. Rev. Lett.*, 1982, **48**, 1425.
24 M. R. Hestenes and E. Stiefel, *J. Res. Natl. Bur. Stand. (U. S.)*, 1952, **49**, 409.
25 J. F. Wolf, B. Vicenzi and H. Ibach, *Surf. Sci.*, 1991, **249**, 233.
26 M. Poensgen, J. F. Wolf, J. Frohn, M. Giesen and H. Ibach, *Surf. Sci.*, 1992, **274**, 430.
27 M. Giesen, *Prog. Surf. Sci.*, 2001, **68**, 1.
28 J.-M. Zhang, X.-L. Xong, X.-J. Zhang, K.-W. Xu and V. Ji, *Surf. Sci.*, 2006, **600**, 1277.
29 X.-L. Zhou and J. M. White, *Catal. Lett.*, 1989, **2**, 375.
30 X.-L. Zhou and J. M. White, *J. Phys. Chem.*, 1991, **95**, 5575.
31 G. J. Szulczewski and J. M. White, *Surf. Sci.*, 1998, **399**, 305.
32 R. S. Mulliken, *J. Chem. Phys.*, 1955, **23**, 1833.
33 W. Wang, X. Shi, S. Wang, M. A. Van Hove and N. Lin, *J. Am. Chem. Soc.*, 2011, **133**, 13264.

